文章编号　2095-1531(2019)02-0405-08

Link performance evaluation for air-sea free-space optical communications

LI Jun[1,2], YUAN Xiu-hua[1,2*], WANG Ming-hao[1,3]

(1. *School of Optical and Electronic Information, Huazhong University of Science and Technology, Wuhan* 430074, *China*;
2. *Institute of Huazhong University of Science and Technology, Shenzhen* 518000, *China*;
3. *Department of Electrical Engineering, Pennsylvania State University, University Park* 16802, *USA*)
* *Corresponding author, E-mail: yuanxh@hust.edu.cn*

Abstract: Effective communication between underwater platforms and aerial platforms has been a challenging issue in a long-time, due to the fact that either acoustic waves or electromagnetic waves can efficiently transmit only in the sea water or air, rather than both. As laser beams are able to penetrate a decent depth of sea water, free-space optical communications (FSOC) is considered to be a good substitutive approach. As is well known, the attenuation caused by absorption and scattering has proved to be the most significant adverse factor for underwater laser propagation, which, however, can only be compensated by a larger power margin. Nonetheless, even if the launching power is large enough to allow for affordable receiver sensitivity, the intensity fluctuation induced by atmospheric and oceanic turbulence can degrade the link performance to a great extent. This study addresses the turbulence effects on FSOC links between an underwater vehicle and an aerial platform. By use of wave optics simulation (WOS), the propagation of both the Gaussian beams and the annular beams in an air-sea two-section link is examined. The difference in performance between the uplink and the downlink is compared and explained according to numerical results. Generally, uplink suffers more from turbulence because the majority of turbulence lies nearer to its transmitter. Moreover, it is found that an annular beam always delivers a smaller scintillation index and a greater signal-to-noise ratio. This study is supposed to benefit the research and development of future air-sea optical communication systems.

Key words: free-space optical communications; annular beams; oceanic turbulence; UUV-UAV optical links; wave optics simulation

收稿日期:2018-05-16;**修订日期**:2018-06-12

基金项目:国家自然科学基金:新型部分相干光束合成机理与方法及其抗大气湍流特性的研究(No. 61275081)
Supported by National Natural Science Foundation of China: Synthesis of Novel Partially Coherent Beams and Research on Their Resilience to Atmospheric Turbulence (No. 61275081)

空潜自由空间光通信的链路性能评估

李　军[1,2],元秀华[1,2*],王铭淏[1,3]
(1. 华中科技大学 光学与电子信息学院,武汉 430074;
2. 华中科技大学 研究院,深圳 518000;
3. 宾夕法尼亚州立大学 电子工程系,大学城 16802)

摘要:长期以来,空中平台与水下平台之间的有效通信一直是一个具有挑战性的课题,因为声波或电磁波只能有效地仅在海水或空气中传播,而无法同时在这两种介质中高效传输数据。相比电磁波,激光束能够穿透相当深度的海水,因而自由空间光通信被认为是一种很好的空潜通信替代手段。众所周知,吸收和散射引起的衰减是水下激光传播主要不利因素之一,然而这只能通过加大发射功率来补偿。尽管如此,即使发射功率大到能够保证一定的接收机灵敏度,大气和海洋湍流引起的光强起伏也会在很大程度上降低链路性能。本文重点研究水下载具与空中平台之间的自由空间光通信链路中的湍流效应,利用波动光学仿真,研究高斯光束和环形光束在空-潜两段链路中的传播,并根据数值结果对上行链路和下行链路之间的性能差异进行了比较说明。总体来说,由于湍流的主要部分离发射机更近,上行链路更容易受到湍流的影响。此外,研究中还发现环形光束往往能产生较小的闪烁指数和较高的信噪比。本项工作能够为未来的空潜光通信系统的研究和发展提供有益的参考。

关　键　词:自由空间光通信;环形光束;海洋湍流;无人水下航行器-无人机光学链路;波动光学仿真
中图分类号:O439　　**文献标识码:**A　　doi:10.3788/CO.20191202.0405

1 Introduction

During the last decade, underwater unmanned vehicles (UUVs) have been widely developed and deployed[1-2], facilitating a variety of offshore and maritime applications. However, the problem arises as how to efficiently exchange information between a UUVs and an unmanned aerial vehicle (UAV) controller. In this case, the UUV cannot be maneuvered remotely by a data cable, as the link is posed as an air-sea two-section wireless link. Traditionally, acoustic waves are used for underwater communications[3-4], but the data rate is restricted to ~100 kbps due to both the low frequency of acoustic carriers and the harsh underwater environment. Moreover, the refraction at the ocean surface makes it highly inefficient for acoustic waves to transmit signals to an above sea platform. On the other hand, whereas electromagnetic waves are prevalent in aerial communications, they are attenuated so fast in sea water that those within 1 meter will be completely absorbed because sea water has much higher electrical conductivity than air.

Optical waves can be considered as a good compromise between their acoustic and electromagnetic counterparts, allowing decent penetrability through sea water as well as high transmission rate. Free-space optical communications (FSOC) has found its position among various modern network infrastructures, while its applications in communications between under water and above water platforms is seldom addressed in literature.

In any aerial optical link, the existence of atmospheric turbulence will inevitably impose wavefront distortion to the propagating laser beam[5-6]. As a result, in the far-field, the beam will be deflected and form optical speckles, leading to intensity fluctuations at the receiver. This is called optical scintillation[7]. The same thing happens for an underwater

optical link, where the turbulence is mainly caused by temperature and salinity gradients. Another major adverse factor in underwater environments is absorption, but since there is no other effective means to compensate for that except to emit more optical power, we will not investigate that aspect here. On the other hand, regardless of the amount of power that is used of the source beam, it is of no help to alleviate the optical scintillation because it is essentially a multiplicative noise. Only by properly designing the spatial properties of the optical source beam can the scintillation be alleviated.

In this study, we will examine the optical link performance between UUVs and low-to-medium altitude UAVs in terms of optical scintillation and signal-to-noise ratio (SNR) at the receiver end. The optical beams considered here are the Gaussian beam and the annular beam. The Gaussian beam is the most commonly used beam type because most lasers´ output conforms to Gaussian profiles, and numerous research papers concerning Gaussian beam turbulence propagation have been published[8-10]. Recent studies also reveal that annular beams are more resilient to turbulence induced intensity fluctuations, indicating it to be potentially better than Gaussian beams in certain application scenarios[11]. Although the study of annular beams propagation in atmospheric slant paths has already been carried out[12-14], no results related to air-sea combined links can be found to date. The performance of the two beam types are compared using wave optics simulation (WOS) numerical method, which is based on fast Fourier transformation (FFT) to compute the Fresnel diffraction integral[15-17]. The turbulence effects are emulated by random phase screens which are arranged to be uniformly distributed for the underwater section of the link. For the aerial part of the link, the phase screens are non-uniformly arranged so as to better reflect the altitude-dependent characteristic of the atmosphere.

The rest of this paper is structured as follows. In Section II the channel model is introduced in a numerical manner and the basics of WOS is briefly explained. Section III provides the simulation results of Gaussian and annular beams propagation through different ranges of air-sea channels, from the perspective of aperture-averaged scintillation and ensembled SNR. Some discussions concerning the obtained results are also included in this part. Section IV is a conclusion and summary of the work presented.

2　Simulation model description

Generally, an optical link between a UUV and a UAV comprises two parts: an underwater section and an aerial section, which is illustrated in Fig. 1. Taking into account the fact that laser beams dissipate within 100m in the sea water, we only consider 50m depth of sea water in the vertical direction. Moreover, recent field-measured data in the Yellow Sea and the Bohai Sea reveal that in autumn and winter the vertical variations of oceanic parameters are almost negligible in the upper layer waters[18], which is why we will model the oceanic turbulence as homogeneous in our case, independent of depth. Therefore, as indicated in Fig. 1, the oceanic turbulence is modeled by equally separated, statistically equivalent phase screens.

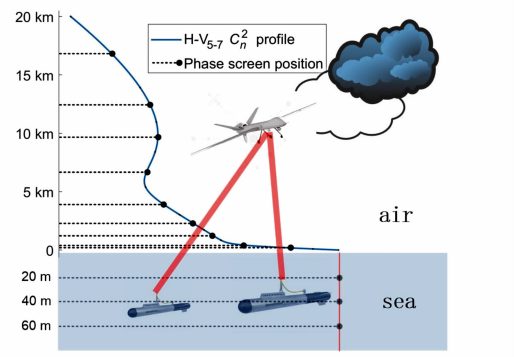

Fig. 1　Air-sea two-section optical link model

The power spectrum density (PSD) model of oceanic refractive index fluctuations adopted here is

the one developed by Nikishov[19], which can be expressed as:

$$\Phi_n(\kappa) = (4\pi)^{-1} C_0 \chi_n \varepsilon^{-1/3} \kappa^{-11/3} [1 + C_1(\kappa\eta)^{2/3}] \varphi(\kappa,\omega) , \quad (1)$$

in which the following denotations have been defined:

$$\varphi_{\text{sea}}(\kappa,\omega) = \frac{\omega^2\theta\exp(-A_T\delta) + \exp(-A_S\delta)}{\omega^2\theta + 1 - \omega(1+\theta)} - \frac{\omega(1+\theta)\exp(-A_{TS}\delta)}{\omega^2\theta + 1 - \omega(1+\theta)}$$

$$\theta = \frac{K_T}{K_S}, \chi_n = \alpha^2\chi_T + \beta^2\chi_S - 2\alpha\beta\chi_{TS}$$

$$\omega = \frac{\alpha(\mathrm{d}T_0/\mathrm{d}z)}{\beta(dS_0/\mathrm{d}z)},$$

$$\delta = 8.284(\kappa\eta)^{4/3} + 12.978(\kappa\eta)^2,$$

among which κ is the spatial wave number, η is the Kolmogorov microscale, and ε is the rate of dissipation of turbulent kinetic energy per unit mass of fluid ranging from 10^{-1} to 10^{-10} $\mathrm{m^2/s^3}$. For constant gradients of mean temperature and salinity, ω defines the ratio of temperature to salinity contributions to the spectrum, varying from -5 (corresponding to temperature dominated turbulence) to 0 (corresponding to salinity dominated turbulence). $C_0 = 0.72$ (the Obukhov-Corrsin constant), C_1 is a free parameter to be determined by comparison with the experiment and its value is taken as 2.35. K_T is eddy thermal diffusivity and K_S is the diffusivity of salt. $A_T = 1.683 \times 10^{-2}$, $A_S = 1.9 \times 10^{-4}$, $A_{TS} = 9.41 \times 10^{-3}$, $\alpha = 2.6 \times 10^{-4}$ L/deg, and $\beta = 1.75 \times 10^{-4}$ L/g. χ_T and χ_S represent the rate of dissipation of mean squared temperature and that of salinity, respectively. χ_{TS} denotes the correlation of χ_T and χ_S.

The phase screen generation process is to randomize the spatial PSD and then FFT it[20].

On the other hand, the altitude-dependent atmosphere density directly leads to a vertically varying atmospheric turbulence profile, for which the best acknowledged model is the H-$V_{5\text{-}7}$, also shown in Fig. 1, where the horizontal scale marks the turbulence strength. To better reflect the unevenness of the H-$V_{5\text{-}7}$ turbulence model and fully utilize the limited computational power, nonuniformly arranged phase screens are used to represent the effects of turbulent wavefront distortions. The partition is based on the path integral of the structure constant and the atmospheric turbulence PSD used here is the modified von Karman spectrum.

$$\varphi_{\text{air}}(\kappa,h) = 0.033 C_n^2(h) \frac{\exp(-\kappa^2/\kappa_l^2)}{(\kappa^2 + \kappa_m^2)^{11/6}} , \quad (2)$$

where $C_n^2(h)$ is the atmospheric refractive index structure constant at altitude h, $\kappa_l = 5.92/l_0$, $\kappa_m = 5.92/L_0$, and where l_0 and L_0 are the inner scale and the outer scale.

The WOS numerical method provides a viable approach to studying complex optical propagation problems. In the scenario considered here, it is nearly impossible to derive analytically expressed results, comprising both underwater and slant-path atmospheric channels, so it is reasonable to use WOS instead. The basic principle of WOS is the split-step propagation between separate phase screens, which can be written as:

$$U_{i+1}(\boldsymbol{r}_{i+1}) = \frac{\exp(jkL/m)}{i\lambda L/m} \cdot \int_S U_i(\boldsymbol{r}_i)\exp[j\psi_i \cdot (\boldsymbol{r}_i)] \exp\left(\frac{jk}{2L/m}|\boldsymbol{r}_{i+1} - \boldsymbol{r}_i|^2\right)\mathrm{d}\boldsymbol{r}_i, \quad i \in [1,m] , \quad (3)$$

where $\boldsymbol{r}$ is the transverse position vector, $U_i(\boldsymbol{r}_i)$ is the optical field at the ith screen, $\psi_i(\boldsymbol{r}_i)$ is the wavefront distortion induced by the turbulence within the ith interval, L is the path length, and m is the number of phase screens. For the specific implementation of WOS, the readers can refer to related literature [20], which we will not reiterate here.

3 Simulation results and discussions

As indicated above, the optical channel that is to be discussed here is a two-section air-sea path,

which is comprised of a 50 m underwater path that is submitted to oceanic turbulence, and a vertical atmospheric path whose length is variable between 1, 2 and 5 km. The optical beams considered here are the Gaussian beam and the annular beam. An annular beam can be represented by the difference of two concentric Gaussian beams[21]. To make these two comparable, the launching power of the annular beam at the source plane is made to be equal to a Gaussian beam with width parameter $w_0 = 50$ mm. Their profiles and the cross-section of the annular beam are shown in Fig. 2.

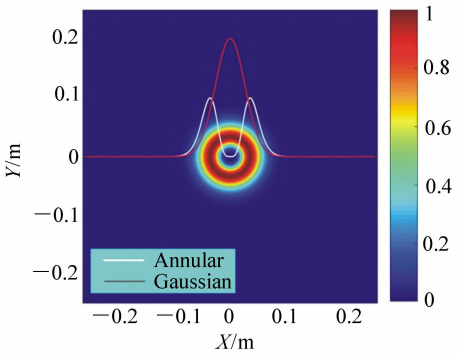

Fig. 2　Comparison of Gaussian beam and annular beam with equal power

In the oceanic turbulence model of Eq. (1), the relevant parameters are set as: $\eta = 2$ mm, $\varepsilon = 10^{-5}$ m^2/s^3, $\omega = -2.5$, $\chi_T = 10^{-8}$ K^2/s. For the von Karman atmospheric spectrum, we have set the inner scale at $l_0 = 5$ mm and the outer scale at $L_0 = 5$ m. In the H-V$_{5\text{-}7}$ model[21], the ground level turbulence strength is $C_n^2(0) = 10^{-5}$ m$^{-2/3}$ and the pseudo wind speed is 27 m/s. Moreover, the wavelength λ is assumed to be 1 μm and 1 000 computation loops are averaged for every single result below. Both the uplink and the downlink are examined.

Fig. 3 shows the beam wander of the Gaussian beam and the annular beam versus the propagation distance. The first thing that should be noted is that it can be found that the downlink beam wander is much less than that of the uplink. This is because in an air-sea optical path, the strongest part of the turbulence lies at the underwater portion and the near sea-level portion, which is close to the uplink transmitter. As a result, the beam is heavily distorted at the beginning of the propagation. During subsequent propagation the distorted wavefront will have enough time to fully diffract and refract, essentially magnifying the earlier imposed distortion. Therefore, in the far-field, the beam exhibits severe beam wander. By contrast, in the downlink the stronger turbulence distortion is imposed to the beam at a relatively later stage of the propagation, leaving less time for the distorted wavefront to evolve, so that the phase distortion does not convert into phase tip and tilt as it does in the case of the uplink.

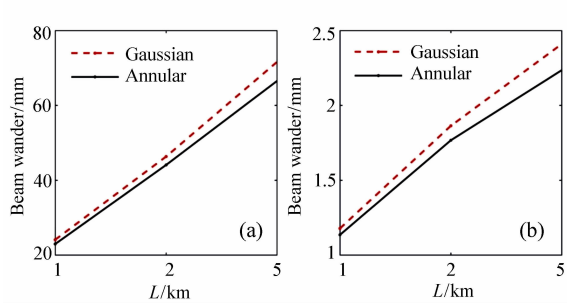

Fig. 3　Beam wanders of the Gaussian beam and the annular beam in (a) uplink, (b) downlink

The other thing that is well worth noting is that in either case, whether it in the uplink or in the downlink, the wanders of annular beam less than that of the Gaussian beam.

For any FSO link, the aperture-averaged scintillation index, also known as irradiance flux variance, is a vital system performance metric[21]. The aperture scintillation indices of the Gaussian beam and the annular beam are compared and the results for three different distances, namely, 1 km, 2 km and 5 km are all provided in Fig. 4. Fig. 4(a)-4(c) is the results for the uplink, where we can see that for the 1 km and the 2 km links, the annular beam always has smaller scintillation once the aperture diameter D is larger than 20 mm. For the 5 km uplink in Fig. 4(c), the annular beam scintillation is significantly reduced compared to that of the Gaussian

beam. For the downlinks, the annular beam seems to be better than the Gaussian beam as well, although the advantage might be minor.

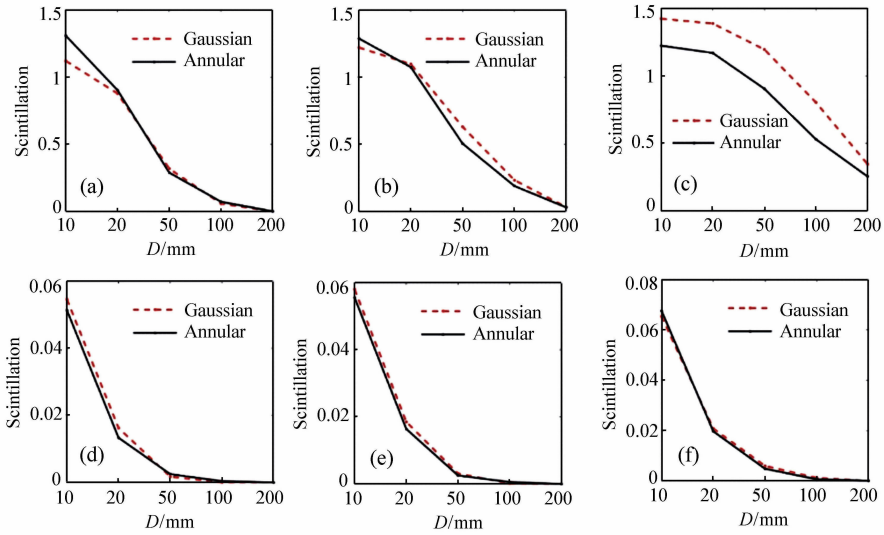

Fig. 4 Scintillation index versus receiver aperture diameter D for (a) 1 km uplink, (b) 2 km uplink, (c) 5 km uplink, (d) 1 km downlink, (e) 2 km downlink, (f) 5 km downlink

Optical scintillation degrades the reliability of the FSO link, which can be evaluated by the probability of fade. Fading is when the received signal level lies below a prescribed threshold. For the case in Fig. 4, the corresponding probability of fade is given in Fig. 5. According to the results, it is safe to say that in the uplink, the annular beam always allows for a smaller probability of fade. For the downlink, if the receiver aperture is not too small, almost no fade would happen.

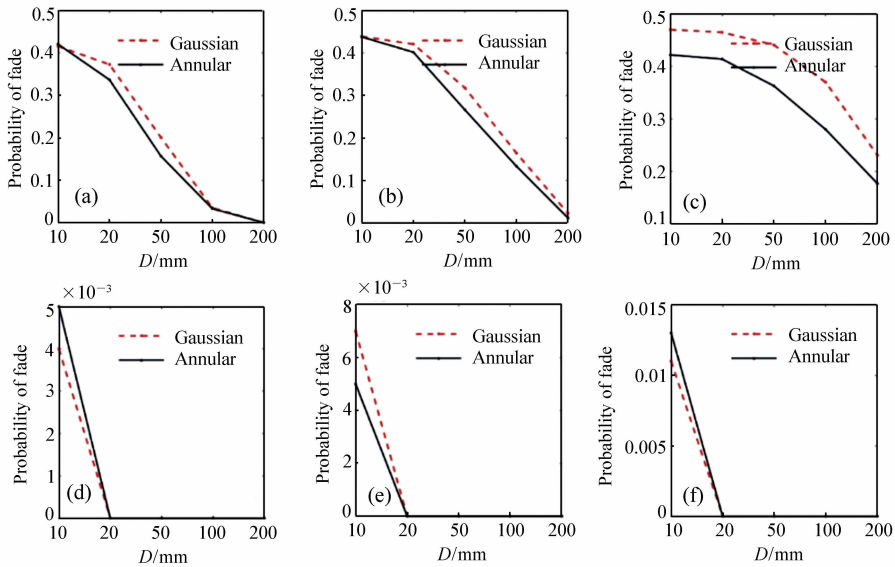

Fig. 5 Probability of fade versus receiver aperture diameter D for (a) 1 km uplink, (b) 2 km uplink, (c) 5 km uplink, (d) 1 km downlink, (e) 2 km downlink, (f) 5 km downlink

Last but not least, the mean SNR is calculated and the results are shown in Fig. 6. Except for the

1 km downlink, the annular beam outperforms the Gaussian beam in terms of SNR.

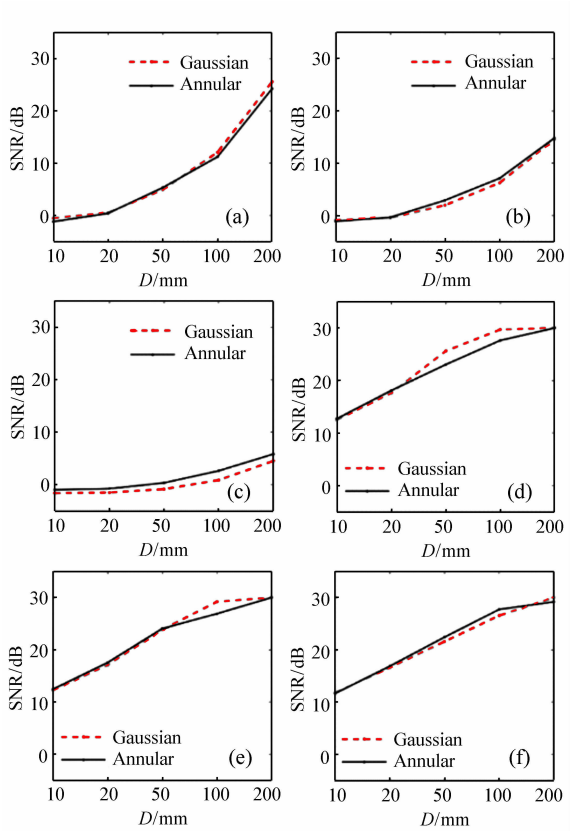

Fig. 6　Mean SNR versus receiver aperture diameter D for (a) 1 km uplink, (b) 2 km uplink, (c) 5 km uplink, (d) 1 km downlink, (e) 2 km downlink, (f) 5 km downlink

4　Conclusion

Using numerical simulation approach, we have presented a study of the optical link evaluation for the air-sea two-section paths between UUVs and UAVs. To our knowledge this is the first time such a type of link configuration is examined in the context of free-space optical communications. The main characteristic of this type of turbulent link is that the turbulence is aggregated at either the transmitter end or the receiver end, forming into an asymmetric phase perturbation structure. In this case, the performance of the Gaussian beam and the annular beam are compared and we can conclude that, under most circumstances, annular beams are obviously a more preferable choice. Generally, in the uplink, beam jitter caused by large-scale turbulence eddies near the transmitter is significantly more severe, leading to worse performance in scintillation, yet the SNR can reach an acceptable level if the receiver aperture is large enough. In the downlink, the degradation caused by turbulence effects is somewhat mild in comparison to that found in the uplink. However, it should be noted that in any air-sea path, the attenuation of the sea water is another major source of the SNR ceiling.

It is also important to notice that the annular beam is quite easy to generate and use, meaning that the switch from Gaussian beams to annular beams will not add much to the overall system cost. Taken that into consideration, combined with the performance improvement that annular beams can provide, as demonstrated by this study, there seems to be no reason to not use annular beams instead of Gaussian beams in FSO systems. This study is supposed to benefit future FSO transceiver designs and implementations.

参考文献:

[1] MAKAVITA C D, JAYASINGHE S G, NGUYEN H D, *et al.*. Experimental study of command governor adaptive control for unmanned underwater vehicles[J]. *IEEE Transactions on Control Systems Technology*, 2019, 27(1): 332-345.

[2] SEDAGHATI S, ABDOLLAHI F, KHORASANI K. Model predictive and non-cooperative dynamic game fault recovery control strategies for a network of unmanned underwater vehicles[J]. *International Journal of Control*, 2017, doi: 10.1080/00207179.2017.1360517.

[3] PREISIG J. Acoustic propagation considerations for underwater acoustic communications network development[C]. ACM International Workshop on Underwater Networks, ACM, 2006: 1-5.

[4] CHITRE M, POTTER J, HENG O S. Underwater acoustic channel characterisation for medium-range shallow water commu-

nications[C]. Oceans '04. MTS/IEEE Techno-Ocean, IEEE, 2004: 40-45.

[5] RATNI B, DE LUSTRAC A, PIAU G P, *et al.*. Reconfigurable meta-mirror for wavefronts control: applications to microwave antennas[J]. *Optics Express*, 2018, 26(3): 2613-2624.

[6] ZHANG D, HAO SH Q, ZHAO Q S, *et al.*. Wavefront reconstruction method based on wavelet fractal interpolation for coherent free space optical communication[J]. *Optics Communications*, 2018, 410: 723-729.

[7] ELAMASSIE M, UYSAL M, BAYKAL Y, *et al.*. Effect of eddy diffusivity ratio on underwater optical scintillation index [J]. *Journal of the Optical Society of America A*, 2017, 34(11): 1969-1973.

[8] BORAH D K, VOELZ D G. Spatially partially coherent beam parameter optimization for free space optical communications [J]. *Optics Express*, 2010, 18(20): 20746-20758.

[9] WANG M H, YUAN X H, MA D L. Potentials of radial partially coherent beams in free-space optical communication: a numerical investigation[J]. *Applied Optics*, 2017, 56(10): 2851-2857.

[10] ZHU X M, KAHN J M. Free-space optical communication through atmospheric turbulence channels[J]. *IEEE Transactions on Communications*, 2002, 50(8): 1293-1300.

[11] GERÇEKCIOĞLU H, BAYKAL Y, NAKIBOĞLU C. Annular beam scintillations in strong turbulence[J]. *Journal of the Optical Society of America A*, 2010, 27(8): 1834-1839.

[12] JI X L, CHEN H, JI G M. Characteristics of annular beams propagating through atmospheric turbulence along a downlink path and an uplink path[J]. *Applied Physics B*, 2016, 122(8): 221.

[13] EYYUBOĞLU H T, ALTAY S, BAYKAL Y. Propagation characteristics of higher-order annular Gaussian beams in atmospheric turbulence[J]. *Optics Communications*, 2006, 264(1): 25-34.

[14] LI X Q, JI X L. Propagation characteristics of decentered annular beams through non-Kolmogorov turbulence[J]. *Journal of the Optical Society of America A*, 2014, 31(1): 172-182.

[15] CYWIAK M, CYWIAK D, YÁÑEZ E. Finite Gaussian wavelet superposition and Fresnel diffraction integral for calculating the propagation of truncated, non-diffracting and accelerating beams[J]. *Optics Communications*, 2017, 405: 132-142.

[16] FESHCHENKO R M, VINOGRADOV A V, ARTYUKOV I A. Propagation of waves from an arbitrary shaped surface-a generalization of the Fresnel diffraction integral[J]. *Optics Communications*, 2018, 413: 291-294.

[17] DWIVEDI G, SHARMA A, DEBNATH S, *et al.*. Comparison of numerical reconstruction of digital holograms using angular spectrum method and Fresnel diffraction method[J]. *Journal of Optics*, 2017, doi: 10.1007/s12596-017-0424-z.

[18] CHEN SH G, ZHANG T L, HU L B, *et al.*. Vertical variations in optical properties of the waters in the Yellow Sea and Bohai Sea at seasonal scales and their influencing mechanisms[J]. *Optics Express*, 2018, 26(4): 4112-4134.

[19] NIKISHOV V V, NIKISHOV V I. Spectrum of turbulent fluctuations of the sea-water refraction index[J]. *International Journal of Fluid Mechanics Research*, 2000, 27(1): 82-98.

[20] SCHMIDT J D. Numerical simulation of optical wave propagation with examples in MATLAB[J]. *Proceedings of SPIE*, 2010, PM199: 212.

[21] ANDREWS L C, PHILIPS R L. *Laser Beam Propagation Through Random Media*[M]. 2nd ed. Bellingham, WA: SPIE, 2005.

Author biographies:

LI Jun (1978—), male, Jingzhou, Hubei. In 2012, he received his master's degree from Yangtze University. Since 2013, he has been a PhD student in School of Optical and Electronic Information at Huazhong University of Science and Technology. Research area: free-space optical communications. E-mail: 52223894@qq.com

YUAN Xiu-hua (1957—), male, Professor at Huazhong University of Science and Technology. Research area: Optical communication device and system technology; Space optical detection technology and new adaptive optics technology; Photoelectric sensing technologies. E-mail: yuanxh@hust.edu.cn